ORGANIC LETTERS

2003
Vol. 5, No. 21
3951−3954

Conformational and Electronic Engineering of Twisted Diphenylacetylenes

Glen Brizius,[†,‡] Kelvin Billingsley,[‡] Mark D. Smith,[‡] and Uwe H. F. Bunz*[,†]

School of Chemistry and Biochemistry, Georgia Institute of Technology, Atlanta, Georgia 30332-0400, and Department of Chemistry and Biochemistry, University of South Carolina, Columbia, South Carolina 29208

uwe.bunz@chemistry.gatech.edu

Received August 13, 2003

ABSTRACT

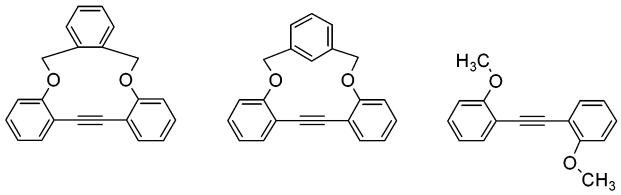

Three tethered diphenylacetylene derivatives were prepared by alkyne metathesis. In these cycles, the twist angle between the two benzene rings is variable and determined by the nature of the linker. The engineering of the twist angle leads to a change of the UV–vis spectra of the cycles. The larger the twist angle in the macrocycles, the more blue shifted their λ_{max} (UV–vis), the lower their fluorescence quantum yield, and the lower field shifted their ^{13}C NMR signals of the alkyne carbons are.

This contribution presents the synthesis of diphenylacetylene derivatives **12**, **13**, and **15** by ring-closing alkyne metathesis. The optical properties of **12**, **13**, and **15** are dependent upon the size of the twist angle α. Increasing the angle α leads to larger HOMO−LUMO gaps and lower emissive efficiencies.

Diphenylacetylenes (DPA) are fascinating in their own right and as building blocks for larger structures, oligo- and poly(phenyleneethynylene)s. DPAs are rigid, and their only degree of freedom is the rotation of the arene units around the central alkyne. This rotational freedom has an impact upon the optical and electronic properties of DPAs **1**−**6** as well upon that of the poly(*p*-phenyleneethynylene)s (PPEs).[1−6]

The conformational change has been invoked to explain the large solvatochromic and thermochromic effects that the PPEs show and the change in fluorescence observed between the pair **1a**/**2** and **2**/**6** upon binding to metal cations.[1] While the PPEs do show large effects in absorption, the DPAs seem to show only a change in emission intensity, but not in their absorption spectra. We found that curious and were interested to "dial in" the twist angle α between the two arene rings in DPAs to examine their electronic properties. There was only sparse information regarding how to change the twist angle in DPAs.[7]

[†] Georgia Institute of Technology.
[‡] Univeristy of South Carolina.

(1) McFarland, S. A.; Finney, N. S. *J. Am. Chem. Soc.* **2002**, *124*, 1178−1179.

(2) (a) Bunz, U. H. F. *Acc. Chem. Res.* **2001**, *34*, 998−1010. (b) Sluch, M. I.; Godt, A.; Bunz, U. H. F.; Berg, M. A. *J. Am. Chem. Soc.* **2001**, *123*, 6447−6448. (c) Levitus, M.; Schmieder, K.; Ricks, H.; Shimizu, K. D.; Bunz, U. H. F.; Garcia-Garibay, M. A. *J. Am. Chem. Soc.* **2001**, *123*, 4259−4265. (d) Miteva, T.; Palmer, L.; Kloppenburg, L.; Neher, D.; Bunz, U. H. F. *Macromolecules* **2000**, *33*, 652−654. (e) Halkyard, C. E.; Rampey, M. E.; Kloppenburg, L.; Studer-Martinez, S. L.; Bunz, U. H. F. *Macromolecules* **1998**, *31*, 8655−8659.

(3) (a) Kim, J.; Levitsky, I. A.; McQuade, D. T.; Swager, T. M. *J. Am. Chem. Soc.* **2002**, *124*, 7710−7718. (b) Kim, J.; Swager, T. M. *Nature* **2001**, *411*, 1030−1034; *Nature* **2001**, *413*, 548 (correction) (c) Zhou, Q.; Swager, T. M. *J. Am. Chem. Soc.* **1995**, *117*, 12593−12603.

(4) Beeby, A.; Findlay, K.; Low, P. J.; Marder, T. B. *J. Am. Chem. Soc.* **2002**, *124*, 8280−8284.

(5) The rotational barrier of tolane is calculated to 0.86 kcal/mol utilizing a B3PW91/6-311G** basis set: Seminario, J. M.; Zacarias, A. G.; Tour, J. M. *J. Am. Chem. Soc.* **1998**, *120*, 3970−3974.

(6) Moore, J. S. *Acc. Chem. Res.* **1997**, *30*, 402−413. Nelson, J. C.; Saven, J. G.; Moore, J. S.; Wolynes, P. G. *Science* **1997**, *277*, 1793−1796.

(7) (a) Crisp, G. T.; Bubner, T. P. *Tetrahedron* **1997**, *53*, 11881−11898. (b) Crisp, G. T.; Bubner, T. P. *Tetrahedron* **1997**, *53*, 11899−11912.

10.1021/ol035532+ CCC: $25.00
Published on Web 09/16/2003

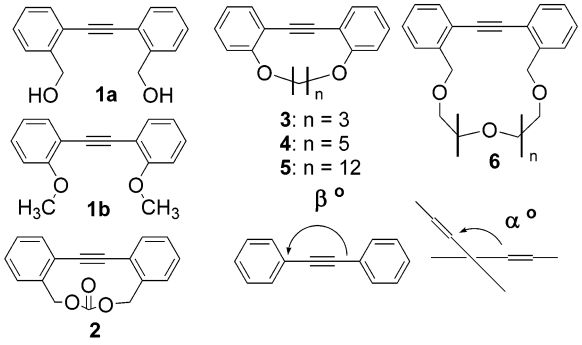

A series of bridged DPAs was checked by us via fast AM1 calculations. Xylylene linkers between the diphenylacetylenes led to structures **12**−**14** with varying α when going from **12** to **14**. Ab initio calculations of these topologies (RHF 6-31G**) refined the picture and showed that **13** is the least twisted cycle (α = 40°) and that both **12** and **14** are considerably more distorted (Figure 1). While these calcula-

Figure 1. Computationally obtained (RHF 6-31G**, Spartan 2002 on a Windows platform) geometries for **12** (left), **13** (middle), and **14** (right). The α values are 58.82°, 39.12°, and 88.02°.

tions give gas phase structures, the 6-31G** basis set is generally reliable for ground-state geometries. Noticeable was the significant shift in the HOMO and LUMO energies upon the twisting action in the three isomeric cycles (Figure 1). While the HOMO−LUMO values do not directly correspond to a physical property they qualitatively match changes in the absorption spectra. An increasing angle α led to an increased HOMO−LUMO gap according to the calculations. Because these cycles are quite flexible, we performed an energy profile calculation with respect to the rotation around the CC triple bond. In **13** and **14,** only one minimum is observed (see Figure 1), but the conformational behavior of **12** is more complex. Two energy minima, one at 0° and one at approximately 60°, are found (Figure 2a). According to different levels of theory either one is somewhat more stable. AM1 and RHF 6-31G** predict the twisted form of **12** to be slightly more stable while B3LYP 6-31G** predicts the planar form of **12** to be more stable. The two conformers are separated by a barrier that was calculated to be between 4 and 7 kcal mol^{-1}. As a comparison, the rotational barrier of **1b** was calculated (Figure 2b). All levels of theory show that the planar syn form in which both methoxy groups are

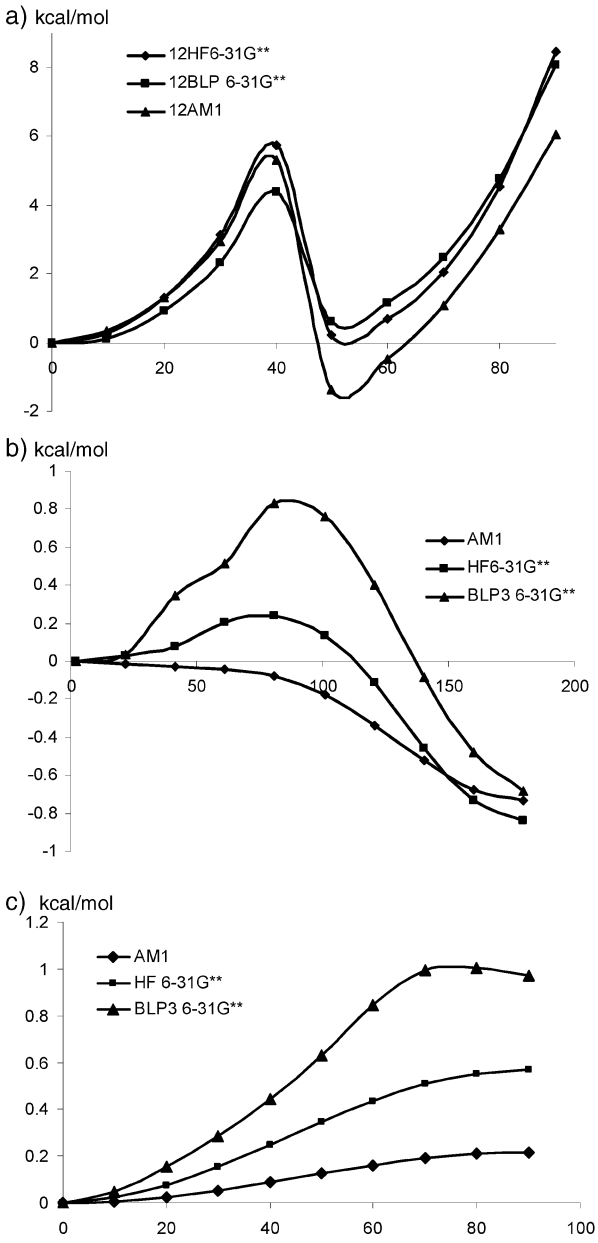

Figure 2. (a) Rotational profile of **12** calculated on three levels of theory. (b) Rotational profile of **1b** calculated on three levels of theory. (c) Rotational profile of diphenylacetylene calculated on three levels of theory. In a−c, the geometry optimization was performed on the AM1 level and the ab initio calculations were single point calculations utilizing optimized AM1 geometries. Abbreviations: HF, restricted Hartree−Fock; BLP, Becke−Lee−Yang−Parr functional (B3LYP). *x*-axis: torsion angle (deg).

located at the same side of the molecule is 0.7−0.8 kcal mol^{-1} less stable than the planar anti form, where both methoxy groups avoid each other. The difference between the calculations is in the height of the barrier, which is nonexistent in the AM1 calculation and approximately 1 kcal mol^{-1} in the DFT calculation.

All of the calculations were single-point energy calculations performed on optimized AM1 geometries. To asses the

precision of these calculations, the rotational barrier of diphenylacetylene was computationally evaluated. This system had been calculated[5] earlier in its planar as well in its 90° twisted conformation. The barrier of rotation was calculated to 0.86 kcal mol^{-1}.[5] When utilizing AM1 optimized geometries and the B3LYP 6-31G** method this barrier is well reproduced with a value of 0.97 kcal mol^{-1}. The relative error utilizing AM1 geometries in combination with single-point ab initio calculations is <0.1 kcal mol^{-1}. The use of AM1-calculated geometries is therefore reasonable. The control calculation backs up the calculational results obtained for **1b** and **12**−**14**.

The synthesis of **12**, **13**, and **15** starts (Scheme 1) with the benzylation of **7** followed by propynylation utilizing a

Scheme 1. Synthesis of Twisted Tolanes

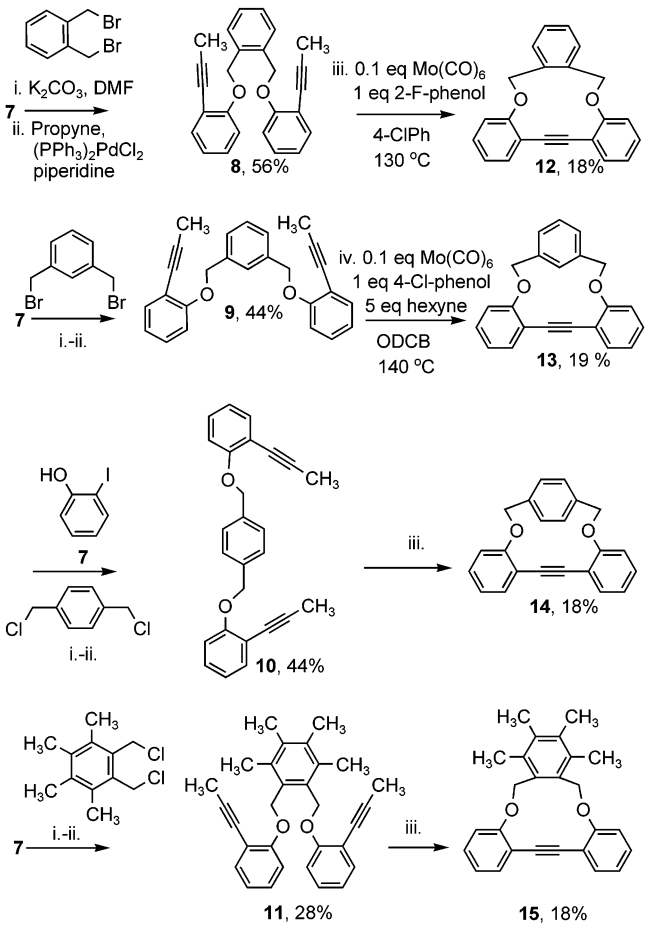

Pd-catalyzed coupling of the Sonogashira type.[8] The bisethers **8**−**11** are isolated in 28−56% yield. Alkyne metathesis with either the Grela[9] system or our own preactivated variant[10] of the Mortreux[11] catalyst furnished the cycles **12**, **13**, and **15** in 18−19% isolated yield after repeated chromatography on silica gel. Major byproducts are scarcely soluble oligomers and polymers that could not be purified/separated. Repeated attempts to close **10** to **14** under different conditions failed with a variety of catalytic in situ systems.

To gain an understanding of the structures of the cycles, we attempted to grow single-crystalline specimens. Cycle **13** is a colorless glass that resisted single-crystal growth. The *ortho* cycles **12** and **15** formed single crystals from hexafluorobenzene (**12**) and hexane/dichloromethane (**15**), respectively. The use of hexafluorobenzene as a crystallization solvent seems critical because it favors aromatic face-to-face interactions.[12−14] The structures of **12** and **15** are shown in Figure 3a,b. There are three independent molecules of **12** in the unit cell. Each of them has a different angle α (22.4−26.6°). The energy potential for rotation is quite soft for **12**, but that is not too unexpected. In the case of **15,** only one twist angle (29.9°) is observed. The twist angle of **12** and **15** in the solid state is significantly smaller than calculated, but this is a packing effect in combination with the soft rotational profile in **12** and **15**. While the X-ray data are an important proof of the topology of the cycles, and show a fascinating solid state ordering, they probably do not correctly represent the conformation of the cycles in solution (Figure 3).

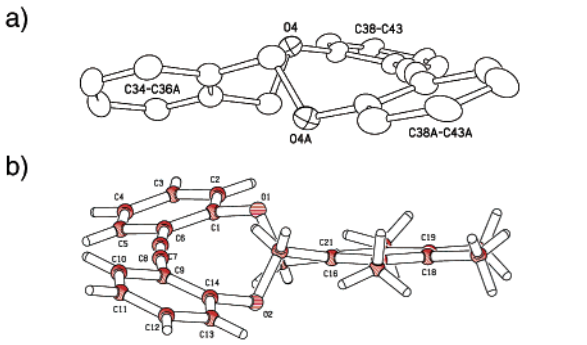

Figure 3. (a) ORTEP representation of **12**; α = 26.6°. (b) Ball and stick representation of **15**; α = 29.9°.

The UV−vis spectra of **12**, **13**, **15**, and **1b** are shown in Figure 4. While **1b** has its λ_{max} at 332 nm, the *ortho* cycles **12** and **15** show their λ_{max} at 313−315 nm, almost 20 nm blue-shifted. All of these spectra display a fine structure. The *meta* cycle **13** features a broad and undistinguished UV−vis spectrum that is intermediate between that of **1b** and the

(8) Bunz, U. H. F. *Chem Rev.* **2000**, *100*, 1605−1644. Sonogashira, K. *J. Organomet. Chem.* **2002**, *653*, 46−49.
(9) Grela, K.; Ignatowska, J. *Org. Lett.* **2002**, *4*, 3747−3749.
(10) (a) Brizius, G.; Bunz, U. H. F. *Org. Lett.* **2002**, *4*, 2829−2831. (b) Kloppenburg, L.; Song, D.; Bunz, U. H. F. *J. Am. Chem. Soc.* **1998**, *120*, 7973−7974.
(11) Mortreux, A.; Blanchard, M. *J. Chem. Soc., Chem. Commun.* **1974**, 786−787. (b) Kaneta, N.; Hikichi, K.; Mori, M. *Chem. Lett.* **1995**, 1055−1066. (c) Kaneta, N.; Hirai, T.; Mori, M. *Chem. Lett.* **1995**, 627−628.
(12) (a) Weck, M.; Dunn, A. R.; Matsumoto, K.; Coates, G. W.; Lobkovsky E. B.; Grubbs, R. H. *Angew. Chem., Int. Ed.* **1999**, *38*, 2741−2744. (b) Coates, G. W.; Dunn, A. R.; Henling, L. M.; Dougherty, D. A.; Grubbs, R. H. *Angew. Chem., Int. Ed. Engl.* **1997**, *36*, 248−251.
(13) Bunz, U. H. F.; Enkelmann, V. *Chem. Eur. J.* **1999**, *5*, 263−266.
(14) (a) Dai, C.; Nguyen, P.; Marder T. B.; Scott, A. J.; Clegg, W.; Viney, C. *Chem. Commun.* **1999**, 2493−2494. (b) Collings, J. C.; Roscoe, K. P.; Robins, E. G.; Batsanov, A. S.; Stimson, L. N.; Howard, J. A. K.; Clark, S. J.; Marder, T. B. *New J. Chem.* **2002**, *26*, 1740−1746.

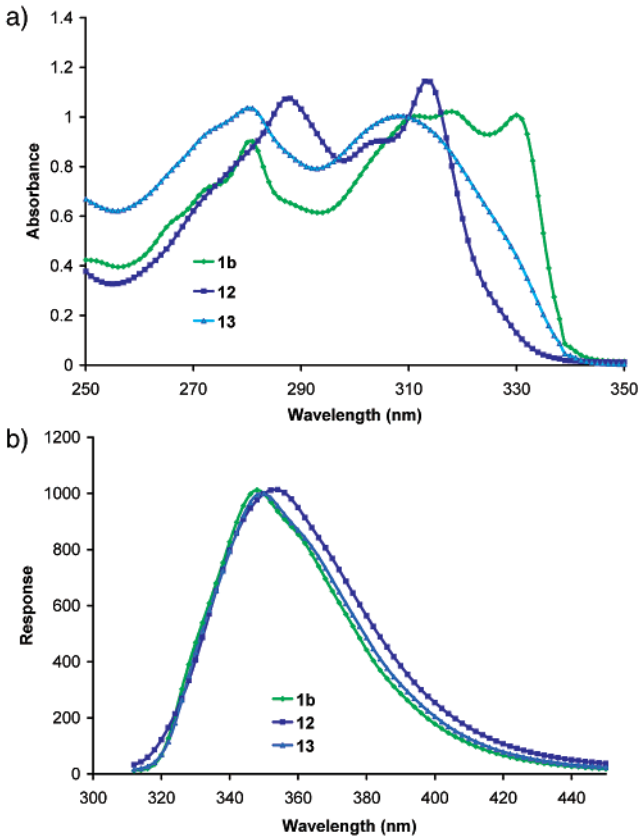

Figure 4. (a) UV−vis spectra (chloroform) of **1b** and the cycles **12** and **13**. (b) Emission spectra (chloroform, height normalized) of **1b** and the cycles **12** and **13**. Emission of **15** is superimposable to that of **12** and therefore not shown.

other cycles. The fine structure in the spectra of **12** and **13** cannot be assigned to any specific vibration(s), and the numeric value of the fine structure in **1b** (2059 cm^{-1}) might be assigned to a CC triple-bond stretch. The fluorescence spectra of **1b** and **12**, **13**, and **15** are similar but their quantum yields are significantly different (Table 1). The fluorescence quantum yield (chloroform) of **13** is 69%, and **12** and **15** feature quantum yields in the range of 10−22%. The parent compound **1b** has a fluorescence quantum yield of 45%. The quantum yields differ considerably upon the solvent utilized, but the trend is unchanged by the choice of solvents. Coinciding with the quantum yields and the blue shift in the absorption are the ^{13}C NMR chemical shifts of the alkyne carbons that deshield in the same way, reaching a maximum of 1.64 ppm in **15**. Again, the meta cycle **13** is the one that resembles **1b** most.

Table 1. Spectroscopic Data of Cycles **12**, **13**, and **15**

	1b	**12**	**13**	**15**
UV−vis ($CHCl_3$, nm)	330	313	309	315
ϵ at λ_{max}		20 000	17 300	21 700
fluorescence (nm)	348	352	350	350
quantum yield ($CHCl_3$)	0.45	0.12	0.69	0.10
CH_2Cl_2	0.75	0.33	0.77	0.21
hexanes	0.54	0.16	0.66	0.08
ethyl ether	0.55	0.15	0.69	0.07
^{13}C NMR alkyne shift, $\triangle$ ppm (**1b**)[a]	0	+1.20	+0.71	+1.64

[a] For the influence of mechanical strain on the ^{13}CNMR spectral shifts of alkynes, see: Lee, D. C.; Sahoo, S. K.; Cholli, A. L.; Sandman, D. J. *Macromolecules* **2002**, *35*, 4347−4355. Cholli, A. L.; Sandman, D. J.; Maas, W. *Macromolecules* **1999**, *32*, 4444−4446.

In conclusion, we have shown that the optical gap and the fluorescence quantum yield in DPAs **1b**, **12**, **13**, and **15** vary in dependence upon the twist angle of the two constituting phenyl rings. A self-consistent picture emerges from experimental and calculational results, in which an increased torsion angle leads to a decreased fluorescence quantum yield *and an enlarged optical gap*.

Acknowledgment. We thank the National Science Foundation (CHE 0138659) and the USC NanoCenter for generous support. U.B. is a Camille Dreyfus Teacher−Scholar (2000−2004).

Supporting Information Available: Experimental procedures and characterization for all compounds and CIFs for **12** and **15**. This material is available free of charge via the Internet at http://pubs.acs.org.

OL035532+